Available online at www.sciencedirect.com
ScienceDirect
Bioorganic & Medicinal Chemistry Letters 18 (2008) 1413–1418
Bioorganic & Medicinal Chemistry Letters

Novel HCV NS5B polymerase inhibitors derived from 4-(1′,1′-dioxo-1′,4′-dihydro-1′λ^6-benzo[1′,2′,4′]thiadiazin-3′-yl)-5-hydroxy-2*H*-pyridazin-3-ones. Part 1: Exploration of 7′-substitution of benzothiadiazine

Yuefen Zhou,* Stephen E. Webber, Douglas E. Murphy, Lian-Sheng Li, Peter S. Dragovich, Chinh V. Tran, Zhongxiang Sun, Frank Ruebsam, Amit M. Shah, Mei Tsan,† Richard E. Showalter, Rupal Patel, Bin Li,‡ Qiang Zhao, Qing Han,§ Thomas Hermann,¶ Charles R. Kissinger, Laurie LeBrun, Maria V. Sergeeva and Leo Kirkovsky

Anadys Pharmaceuticals, Inc., 3115 Merryfield Row, San Diego, CA 92121, USA

Received 9 November 2007; revised 23 December 2007; accepted 2 January 2008
Available online 8 January 2008

Abstract—5-Hydroxy-3(2*H*)-pyridazinone derivatives were investigated as inhibitors of genotype 1 HCV NS5B polymerase. The synthesis, structure–activity relationships (SAR), metabolic stability, and structure-based design approach for this new class of compounds are discussed.

Hepatitis C virus (HCV) infection is a major health problem worldwide and is a leading cause of liver disease. It is estimated that over 170 million people are infected with HCV with 3–4 million individuals becoming newly infected each year.[1] The current standard therapy is a combination of pegylated interferon (peg-IFN) and ribavirin (RBV). Unfortunately, response rates to this therapy are sub-optimal and are particularly low in patients infected with genotype 1 HCV.[2] In addition, this standard of care is often associated with significant side effects.[2] The drawbacks of current HCV therapy necessitate the development of more effective anti-HCV agents, especially for treatment of patients infected with genotype 1 HCV.

The HCV NS5B protein is a virally encoded RNA-dependent RNA polymerase (RdRp), the activity of which is critical for the replication of the virus.[3] Inhibitors of this enzyme therefore have potential to become novel direct antiviral agents for the effective treatment of HCV infection. Several nucleoside and non-nucleoside NS5B inhibitors are currently in clinical trials.[4] Most non-nucleoside NS5B inhibitors are known to bind to one of three allosteric pockets of the protein that are distinct from the active site.[4a] Our computational analysis of these pockets indicated that a binding site at the palm domain was highly conserved across various genotype 1 HCV sequences. We therefore concentrated our efforts on the development of non-nucleoside small molecule inhibitors of genotype 1 HCV NS5B polymerase which bind at this location.

Keywords: Pyridazinones; 5-Hydroxy-3(2*H*)-pyridazinone derivatives; Hepatitis C virus (HCV); Structure-based design; RNA-dependent RNA polymerase (RdRp); Small molecule, Non-nucleoside NS5B inhibitors.
* Corresponding author at present address: Anadys Pharmaceuticals, Inc., 3115 Merryfield Row, San Diego, CA 92121, USA. Tel.: +1 858 530 3693; fax: +1 858 530 3644; e-mail: yzhou@anadyspharma.com
† Present address: Illumina, 9885 Towne Centre Drive, San Diego, CA 92121-1975, USA.
‡ Present address: Shanghai ChemPartner Co., Ltd, No. 3 Building, 720 Cailun Road, Pudong, Shanghai 201203, China.
§ Present address: Structure Based Design, Inc., 5560 Lusk Blvd. B104, San Diego, CA 92121, USA.
¶ Present address: Department of Chemistry and Biochemistry, University of California, San Diego, 9500 Gilman Drive, La Jolla, CA 92093-0358, USA.

0960-894X/$ - see front matter © 2008 Elsevier Ltd. All rights reserved.
doi:10.1016/j.bmcl.2008.01.007

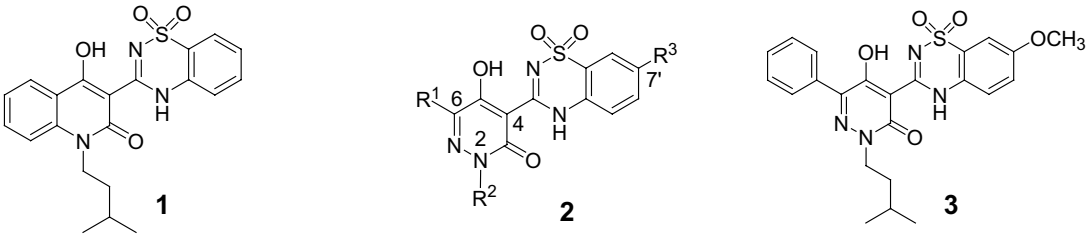

Figure 1. HCV NS5B polymerase inhibitors.

Several classes of inhibitors are known to bind at the NS5B palm site.[4e,5,6] Of these, compound **1**, containing the 1,1-dioxo-benzo[1,2,4]-thiadiazine moiety, exhibits potent NS5B inhibition (Fig. 1).[6] As evident from the X-ray co-crystal structure of compound **1** bound to the NS5B polymerase, this class of molecules has a relatively planar conformation with a minor (20°) rotation between the quinolinedione and benzothiadiazine rings governed by intramolecular H-bonding.[6] These structural features are highly favorable for binding to the NS5B palm site. However, we reasoned that they may lead to some undesirable pharmaceutical properties including poor aqueous solubility. We envisioned that removing the fused benzene ring from the quinolinedione core could afford a molecule with increased flexibility and reduced lipophilicity to improve overall physicochemical properties. Therefore, we were interested in replacing the quinolinedione core of compound **1** with a 5-hydroxy-3(2*H*)-pyridazinone, leading to structures of type **2**. We were encouraged by the modest NS5B inhibition activity displayed by an early lead compound **3**.

The co-crystal structure of compound **3** bound to the NS5B protein was determined in order to facilitate our subsequent lead optimization process (Fig. 2). The co-crystal structure revealed several tightly bound water molecules surrounding compound **3**. Two of these water molecules mediated important hydrogen bonds between the inhibitor and the protein. One water molecule bridged a sulfonamide O-atom to the NS5B residues Ser556 and Ser288, while the other formed H-bonds between the pyridazinone enolic OH and amino acid residue Gly449. These H-bond networks are believed to be an important contributing factor for NS5B binding affinity. In addition, the pyridazinone and benzothiadiazine rings in compound **3** adopted a geometry that was within 25° of being co-planar, similar to the corresponding orientation observed between the quinolinedione and benzothiadiazine moieties of compound **1**.[4a] Another key feature of the co-crystal structure was a deep hydrophobic pocket in the enzyme that was occupied by the R^2 isoamyl group. The R^1 phenyl ring filled a somewhat shallow cavity in proximity to the Met414 side chain by rotating up to 45° out of plane relative to the pyridazinone ring. The geometry of the R^1 phenyl group suggested that a smaller ring, such as a thiophene moiety, might be better accommodated in this region. The methoxy R^3 substituent of **3** was deemed to be sub-optimal due to a lack of appropriate space filling. However, the oxygen atom at 7′-position could be further elaborated to increase the NS5B binding affinity

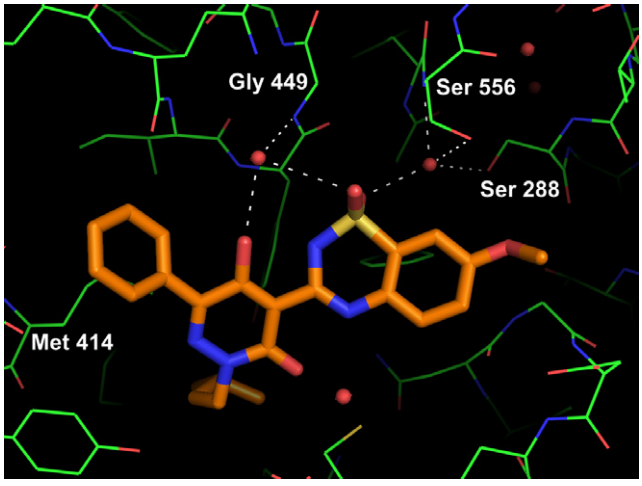

Figure 2. Co-crystal X-ray structure of compound **3** bound to the NS5B protein (2.65 Å).[7] Apparent hydrogen bond interactions with N- and O-atoms with distance less than 3.2 Å and favorable geometries are shown as dashed lines.

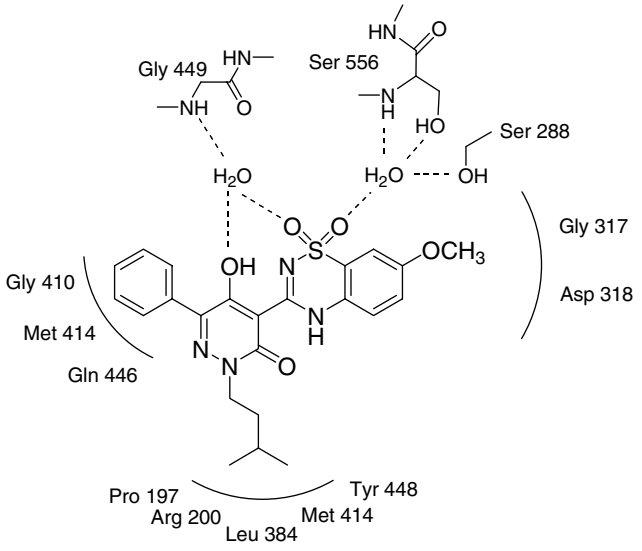

Figure 3. Schematic diagram of compound **3** bound in the NS5B palm site. Hydrogen bonds are represented as dashed lines, and the residues which make up the enzyme binding subsites are depicted.[8]

by filling up more space in the R^3 region of the binding pocket. A schematic diagram shown in Figure 3 summarizes the interactions observed in the co-crystal structure of compound **3** complexed with the NS5B protein.

In order to systematically explore the SAR of the R^1, R^2, and R^3 substituents to optimize this series of compounds, several methods were developed to synthesize compounds **2**. Of these, methods A and B are the most preferred approaches to construct the core structure of **2** as shown in Scheme 1.[9]

When method A was used, 5-hydroxy-3-oxo-pyridazine-4-carboxylic acid ethyl esters (**4**)[9,10] were condensed with 2-amino-sulfonamides (**5**)[11] in pyridine at 120 °C to form amide intermediates which underwent cyclization in the presence of DBU to give the desired products (**2**). When method B was applied, DCC-mediated coupling of hydrazone (**6**)[10] with carboxylic acids (**7**)[11] at room temperature afforded amide intermediates which were cyclized under basic conditions using Et_3N or a 21% w/w solution of NaOEt in EtOH to give the desired products (**2**). Both methods furnished **2** with reasonable yields (20–65%).

We started our lead optimization efforts by replacing the R^1 phenyl ring present in compound **3** with a 2-thiophene moiety while keeping the R^2 and R^3 substituents unchanged (**8a**, Table 1). This modification afforded a 9-fold improvement in NS5B inhibition activity as compared with the lead compound **3**. This result is consistent with the X-ray structure analysis of compound **3** complexed with the NS5B protein. We then kept 2-thiophene as R^1 and isoamyl as R^2 constant but varied R^3 to study the SAR at this position. The inhibitory activities against genotype 1b in both enzyme and cell culture replicon assays were measured. In addition, the stability of the compounds toward human liver microsomes (HLM) was determined. The data are listed in Table 1.

Removal of the methoxy R^3 substituent present in **8a** led to a 3-fold increase in NS5B inhibition activity (**8b**), and its replacement with a hydroxyl moiety (**8c**) significantly improved enzyme inhibition properties. Importantly, extension of the R^3 substituent along with the addition of a polar acetamide group at its terminus afforded a compound (**8d**) with substantially improved enzyme inhibition activity. This molecule also exhibited good antiviral potency in the replicon cell culture assay that was clearly distinct from cytotoxicity. The significant increase in potency (>50-fold) for **8d** compared with **8a** can likely be attributed to the formation of additional hydrogen bonds between the acetamide moiety and the NS5B protein. Such interactions were observed in the crystal structure of **8d** complexed with the NS5B protein (Fig. 4). They involved the terminal NH of the acetamide moiety and amino acid residues Asp318 and Asp225 (via water molecules) as well as the acetamide O-atom and residues Asn291 and Asp225 (via another water molecule) of the NS5B protein. In addition, the increased length of the OCH_2CONH_2 (required for filling the space in the R^3 region of the binding pocket) may also contribute to the increased affinity.

Analysis of the **8d**-NS5B co-crystal structure suggested that small alkyl groups could be appended to one face of the R^3 methylene moiety present in **8d** without negatively impacting NS5B interactions. Accordingly, we introduced a single methyl group at this location with the expectation that this modification might reduce the polarity of the R^3 moiety and increase cell permeability. The resulting compound (**8e**) exhibited equipotent NS5B inhibition in enzyme assays compared with the non-methylated analog **8d**, and displayed comparable cellular activity. The X-ray crystal structure of **8e** complexed with the NS5B protein in the R^3 region clearly showed that the R^3 conformation and interactions with the NS5B protein were very similar to that of **8d** (Fig. 4).

In addition, as anticipated from the **8d**-NS5B co-crystal structure, substitution with a geminal dimethyl moiety or larger alkyl groups (**8f** and **8g**, respectively) resulted in a significant loss of NS5B inhibition activity.

Analysis of the **8d**-NS5B co-crystal structure also suggested that the R^3 acetamide moiety would tolerate the

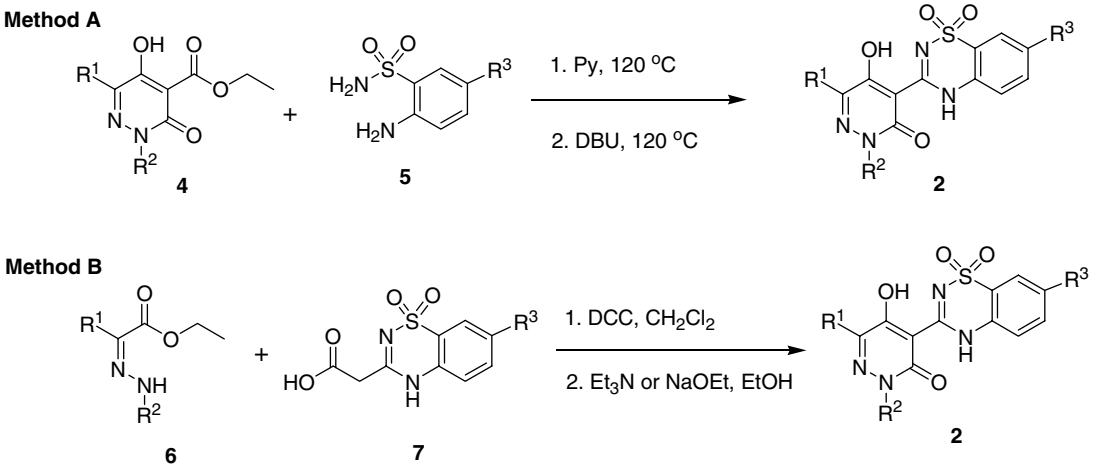

Scheme 1. General methods for the synthesis of pyridazinone derivatives (**2**).

Table 1. Pyridazinone NS5B inhibitors with O-linked R^3 substituents

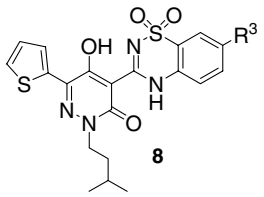

8

Compound[a]	R^3	IC_{50} (1b), μM[b]	EC_{50} (1b), μM[c]	CC_{50} (GAPDH), μM[c]	HLM $t_{1/2}$ (min)[d]
8a	OMe	3.8	26	78	10
8b	H	1.3	7.1	>33	12
8c	OH	0.34	6.5	>25	5.6
8d	OCH_2CONH_2	0.07	0.41	78	23
8e[e]	$OCH(Me)CONH_2$	0.062	0.21	68	13
8f	$OC(Me)_2CONH_2$	1.6	8.2	>33	21
8g[e]	$OCH(Et)CONH_2$	1.55	7.6	>33	21
8h	$OCH_2CONHCH_3$	0.092	0.71	>33	20
8i	$OCH_2CONHOH$	0.1	1.1	>33	>60
8j	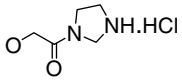	0.34	2.1	>100	42
8k[e]	$OCH(Me)CO_2Et$	6.3	>10	>10	25
8l[e]	$OCH(Me)CO_2H$	0.37	53	>100	>60
8m	OCH_2CN	0.57	0.54	>33	15

[a] See Ref. 12.
[b] See Ref. 13.
[c] See Ref. 14.
[d] See Ref. 15.
[e] Racemic.

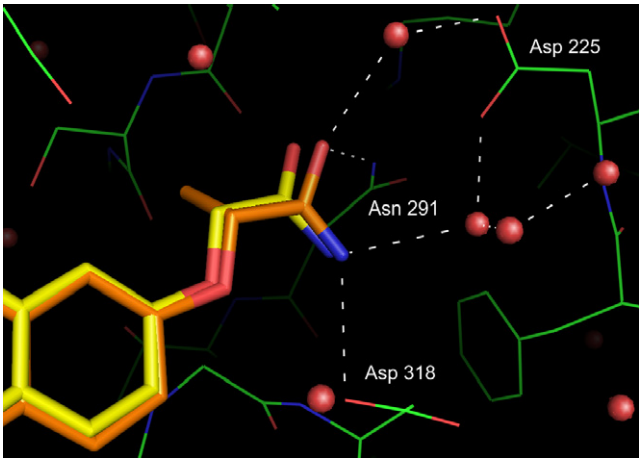

Figure 4. The overlay of X-ray crystal structures of **8d** (2.4 Å, yellow carbon) and **8e** (2.3 Å, orange carbon) complexed with the NS5B protein highlighting the R^3 region.[7]

addition of small appendages to its terminus. This hypothesis was confirmed by the preparation of the corresponding N-methylated compound **8h** and the hydroxamic acid derivative **8i** which both displayed comparable NS5B inhibition activities to that exhibited by **8d**. Interestingly, alkylation of the polar NH_2 group of **8d** with the expectation of possibly enhancing cell permeability[16] did not improve the compound's antiviral properties ($EC_{50}/IC_{50} \cong 6$–8 for both compounds **8h** and **8d**). The inclusion of a larger cyclic moiety at the R^3 terminus (**8j**) diminished the enzyme inhibition activity by 5-fold compared with **8d**, which was consistent with our prediction based on the **8d**-NS5B co-crystal structure.

Furthermore, replacement of the terminal amide moiety with an ester significantly reduced NS5B inhibitory potency (compare **8k** with **8e**) likely due to the loss of the hydrogen bonds formed between the **8e** R^3 terminal NH moiety and the NS5B protein. In addition, the larger R^3 ethyl ester group may be too voluminous to fit well in the binding pocket. However, the inhibition activity could be partially restored by incorporation of the corresponding carboxylic acid moiety into the terminal R^3 group (as in compound **8l**). This result may be due to the reduction in size of the R^3 group and the possible formation of hydrogen bonds between the OH group of the carboxylic acid and the surrounding NS5B residues.

Other modifications of the R^3 substituents, that are either C- or N-linked to the benzothiadiazine ring at the 7′-position (**8n**–**8y**), are summarized in Table 2. None of the variations including ketones, amides, heteroaromatics, and cyano moieties led to any improve-

Table 2. Pyridazinone NS5B inhibitors with C- and N-linked R^3 substituents

Compound[a]	R^3	IC_{50} (1b), μM[b]	HLM $t_{1/2}$ (min)[c]
8n	$CH_2CH_2CONH_2$	3.4	>60
8o	$CH{=}CHCONH_2$	0.23	31
8p	NHCO-*c*-Pr	8	5.0
8q	$NHCOCH_3$	1.1	3.3
8r	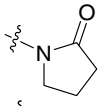	7.2	4.3
8s[e]	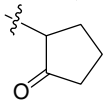	11	44
8t	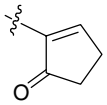	5.3	3.6
8u	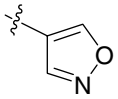	2.1	30
8v	$COCH_3$	2.5	4.3
8w	CN	0.71	9.6
8x	$CONH_2$	0.58	3.7
8y		0.29	16

[a] See Ref. 12.
[b] See Ref. 13.
[c] See Ref. 15.
[d] Not determined.
[e] Racemic.

ment in NS5B inhibitory potency as compared with compounds **8d** or **8e**. Therefore, no further evaluation was performed on these molecules other than metabolic stability assessment. The difference in activity of **8d**, **8o**, and **8n** could be explained by the difference in the preferred conformation of the R^3 groups. To allow for the favorable hydrogen bonding interactions (Fig. 4), the R^3 group needs to be close to co-planar to the benzothiadiazine ring. In **8d** and **8o** this is the preferred conformation. However, in **8n** the lowest energy conformation will have the second methylene group rotated out of the plane of the aromatic system.

In anticipation of assessing the in vivo PK properties of potent pyridazinone-containing NS5B inhibitors, we also examined the stability of these compounds toward human liver microsomes (HLM). As shown in Tables 1 and 2, the measured HLM half-lives for a majority of the compounds (**8a**–**h**, **8k**, **8m**, **8p**–**r**, **8t**, **8v**–**y**) were relatively short (<30 min). However, compounds **8j** and **8s** bearing either a polar cyclic acetamide moiety via an O-linkage or a cyclic ketone group via a C-linkage exhibited moderate half-lives (42 and 44 min, respectively). The most stable compounds (**8i**, **8l**, and **8n**) possessed a hydroxamic acid or a carboxylic acid or a C-linked acetamide moiety and exhibited long half-lives (>60 min). These results implied that the very hydrophilic pyridazinone compounds might have poor/non-productive interactions with CYPs and suggested that R^3 substitution could impact the human liver microsomal stability of the molecules under study.

In summary, we discovered a new class of 4-(1′,1′-dioxo-1′,4′-dihydro-1′. λ^6-benzo[1′,2′,4′]thiadiazin-3′-yl)-5-hydroxy-2*H*-pyridazin-3-one derivatives as potent inhibitors of genotype 1b HCV NS5B polymerase using a structure-based design approach. The synthesis of this new class of pyridazinone compounds was developed with reasonable yields using either methods A or B. In addition, optimization of the R^3 substituents in this series resulted in NS5B inhibitors with sub-micromolar potencies in both biochemical and cell culture replicon assays. Furthermore, the R^3 substitution also affected the stability of the molecules toward human liver microsomes. In a separate communication, we will describe the SAR of R^1 and R^2 substituents in this series focusing on potency and HLM stability.[17]

Acknowledgments

The authors thank Drs. Devron Averett and Steve Worland for their support and helpful discussions during the course of this work. The authors also thank Dr. Alberto Gobbi for the computational chemistry discussion.

References and notes

1. (a) Kim, W. R. *Hepatology* **2002**, *36*, 30; (b) Alter, M. J.; Kruszon-Moran, D.; Nainan, O. V.; McQuillan, G. M.; Gao, F.; Moyer, L. A.; Kaslow, R. A.; Margolis, H. S. *N. Engl. J. Med.* **1999**, *341*, 556.
2. Hoofnagle, J. H.; Seeff, L. B. *N. Engl. J. Med.* **2007**, *355*, 2444.
3. Kolykhalov, A. A.; Agapov, E. V.; Blight, K. J.; Mihalik, K.; Feinstone, S. M.; Rice, C. M. *Science* **1997**, *277*, 570.
4. (a) Koch, U.; Narjes, F. *Curr. Top. Med. Chem.* **2007**, *7*, 1302; (b) Pierra, C.; Benzaria, S.; Amador, A.; Moussa, A.; Mathieu, S.; Storer, R.; Gosselin, G. *Nucleosides, Nucleotides Nucleic Acids* **2005**, *24*, 767; (c) Pierra, C.; Amador, A.; Benzaria, S.; Cretton-Scott, E.; D'Amours, M.; Mao, J.; Mathieu, S.; Moussa, A.; Bridges, E. G.; Standring, D. N.; Sommadossi, J.-P.; Storer, R.; Gosselin, G. *J. Med. Chem.* **2006**, *49*, 6614; (d) Conference report from the 57th Annual Meeting of the American Association for the Study of Liver Diseases (AASLD), October 27–31, 2006, Boston, MA, http://www.natap.oeg/2006/AASLD/AASLD_04.htm; (e) Slater, M. J. et al. *J. Med. Chem.* **2007**, *50*, 897; (f) Conference report from 42nd Meeting of the European Association for the Study of Liver Diseases (EASL), April 11–15, 2007, Barcelona, Spain, http://www.natap.org/2007/EASL/EASL_13.htm;; (g) Conference report from Digestive Disease Week, Los Angeles, May 21–24, 2006, http://www.natap.org/2006/DDW/DDW_18.htm.
5. (a) Dhanak, D. et al. *J. Biol. Chem.* **2002**, *277*, 38322; (b) Evans, K. A.; Chai, D.; Graybill, T. L.; Burton, G.; Sarisky, R. T.; Lin-Goerke, J.; Johnston, V. K.; Rivero, R. A. *Bioorg. Med. Chem. Lett.* **2006**, *16*, 2205; (c) Blake, J. F.; Fell, J. B.; Fischer, J. P.; Hendricks, R. T.; Spencer, S. R.; Stengel, P. J. WO2006117306, 2006; (d) Pratt, J. K.;

Donner, P.; McDaniel, K. F.; Maring, C. J.; Kati, W. M.; Mo, H.; Middleton, T.; Liu, Y.; Ng, T.; Xie, Q.; Zhang, R.; Montgomery, D.; Molla, A.; Kempf, D. J.; Kohlbrenner, W. *Bioorg. Med. Chem. Lett.* **2005**, *15*, 1577; (e) Hutchinson, D. K. et al. U.S. Patent US2005107364, bf 2005.

6. Tedesco, R.; Shaw, A. N.; Bambal, R.; Chai, D.; Concha, N. O.; Darcy, M. G.; Dhanak, D.; Fitch, D. M.; Gates, A.; Gerhardt, W. G.; Halegoua, D. L.; Han, C.; Hofmann, G. A.; Johnston, V. K.; Kaura, A. C.; Liu, N.; Keenan, R. M.; Goerke, J. L.; Sarisky, R. T.; Wiggall, K. J.; Zimmerman, M. N.; Duffy, K. J. *J. Med. Chem.* **2006**, *49*, 971.
7. Crystals of HCV NS5B polymerase (genotype 1b, strain BK, Δ21) were grown by the hanging drop method at room temperature using a well buffer of 20% PEG 4K, 50 mM ammonium sulfate, 100 mM sodium acetate, pH 4.7, with 5 mM DTT. The crystals formed in space group $P2_12_12_1$ with approximate cell dimensions, $a = 85$ Å, $b = 106$ Å, $c = 127$ Å containing two protein molecules in the asymmetric unit. Protein–inhibitor complexes were prepared by soaking these NS5B crystals for 3–24 h in solutions containing 15–20% DMSO, 20% glycerol, 20% PEG 4K, 0.1 M HEPES, 10 mM $MgCl_2$ at pH 7.6, and inhibitors at concentrations of 2–10 mM. Diffraction data were collected to a resolution of 2.65 Å for compound **3** and 2.3 Å for compound **8e**. Diffraction data for **8e** were collected on beamline 14IDB at the Advanced Photon Source at Argonne National Laboratory. Crystal structures discussed in this paper have been deposited in the Protein Databank (www.rcsb.org) with entry codes: 3BSC and 3BR9. Full details of structure determination are given in the respective PDB entries.
8. The O-atom at the 5-position of the pyridazin-3-one in Figure 3 was arbitrarily drawn in the protonated form. The precise extent of the protonation was not determined.
9. The procedures for the synthesis of 5-hydroxy-3(2*H*)-pyridazinone derivatives (**2**) using methods A and B (and other methods) are described in Zhou, Y.; Li, L.-S.; Webber, S. E. WO06066079A2, 2006.
10. The procedures for the synthesis of pyridazinone esters **4** and hydrazones **6** are described in (a) Li, L.-S.; Zhou, Y.; Zhao, J.; Dragovich, P. S.; Stankovic, N. S.; Bertolini, T. M.; Murphy, D. E.; Sun, Z.; Tran, C. V.; Ayida, B. K.; Ruebsam, F.; Webber, S. E. *Synthesis* **2007**, 3301; (b) Murphy, D. E.; Dragovich, P. S.; Ayida, B. K.; Bertolini, T. M.; Li, L.-S.; Ruebsam, F.; Stankovic, N. S.; Sun, Z.; Zhou, Y. *Tetrahedron Lett.* **2008**, *49*, 811.
11. 2-Amino-sulfonamides **5** and benzothiodiazine acids **7** where R^3 is OMe were prepared using modified literature methods as described in (a) Fitch, M. D.; Evans, K. A.; Chai, D.; Duffy, K. J. *Org. Lett.* **2005**, *7*, 5521; (b) Kovalenko, S. N.; Chernykh, V. P.; Shkarlat, A. E.; Ukrainets, I. V.; Gridasov, V. I.; Rudnev, S. A. *Chem. Heterocycl. Compd. (Engl. Transl.)* **1999**, *34*, 791.
12. The structures of all compounds were consistent with ^{1}H NMR and LC–MS data (⩾95% HPLC purity). They are arbitrarily drawn in one tautomer form.
13. NS5B polymerase inhibition assay (IC_{50}, μM): Assays were performed in a 96-well streptavidin-coated FlashPlate using 20 nM enzyme (Δ21 Consensus 1b), 0.5 μCi of [α-^{33}P]GTP, 0.6 μM GTP, and 250 nM 5′biotinylated oligo (rG_{13})/poly rC in 20 mM Tris–HCl, pH 7.5, 20 mM NaCl, 5 mM $MgCl_2$, 5 mM dithiothreitol, 0.1 g/L bovine serum albumin, and 100 U/mL RNAse inhibitor, with inhibitor concentration varied over a suitable range, and with total DMSO at 2% (V/V). The reaction was stopped by aspiration after 75 min at 28 °C and the plate was washed several times with 150 mM NaCl aqueous solution. After washing and drying the plate, incorporated radioactivity was counted using a Microbeta scintillation counter. IC_{50} values were calculated relative to the uninhibited control and inhibition data were fitted to a 4-parameter IC_{50} equation. The estimated average standard deviation for IC_{50} data is 32% from the mean value.
14. HCV replicon assay (EC_{50}, μM): The cell culture component of the assay was performed essentially as described by Bartenschlager et al. *Hepatology* **2002**, *35*, 694, wherein exponentially growing HCV Huh-7/C24 replicon cells were seeded at 4.5×10^3 cells/well in 96-well plates and 24 h later were treated with eight point half-log concentration of compound. After 72 h exposure, the media were discarded from the compound assay plate and the cell monolayers were lysed by addition of 150 μL lysis mixture (Genospectra) with incubation at 53 °C for 45 min. Following incubation, each lysate was thoroughly mixed and 5 μL (NS3 probe) or 10 μL (GAPDH probe) of each lysate was then transferred to the capture plate and analyzed by bDNA assay to determine the EC_{50} and CC_{50} values, respectively. The estimated average standard deviation for EC_{50} data is 56% from the mean value.
15. Human liver microsomal half-life (HLM $t_{1/2}$) assay conditions: The final concentrations in the assay were 0.5 mg/mL microsomes, 5 μM test article (except **8r** with 3 μM), 3.3 mM glucose-6-phosphate, 1.3 mM $NADP^+$, and 0.4 U/mL glucose-6-phosphate dehydrogenase in 50 mM potassium phosphate (pH 7.4) and 3.3 mM $MgCl_2$ buffer. Samples were incubated at 37 °C. At 0, 5, 10, 20, 30, 45, and 60 min, the reactions were terminated by removing 125-μL aliquots and quenching the reaction mixture in 375 μL of ACN. The samples were vortexed and centrifuged. The supernatant was removed and dried under nitrogen. The dried samples were reconstituted in 2% DMSO in water and analyzed by LC/MS/MS for the remaining parent molecules. The $t_{1/2}$ values were determined by fitting the data to a single exponential decay curve. Comparison of $t_{1/2}$ values from multiple replicate experiments on a representative compound gave a 16% standard deviation from the mean value.
16. Conradi, R. A.; Hilgers, A. R.; Ho, N. F. H.; Burton, P. S. *Pharm. Res.* **1992**, *9*, 435.
17. Zhou, Y.; Li, L.-S.; Dragovich, P. S.; Murphy, D. E.; Tran, C. V.; Ruebsam, F.; Webber, S. E.; Shah, A. M.; Tsan, M.; Averill, A.; Showalter, R. E.; Patel, R.; Han, Q.; Zhao, Q.; Hermann, T.; Kissinger, C. R.; LeBrun, L.; Sergeeva, M. V. *Bioorg. Med. Chem. Lett.* **2008**, *18*, 1419.